

Investigation of double beta decay with the NEMO-3 detector

A.S. Barabash,^{1,*} V.B. Brudanin,² and NEMO Collaboration

¹*Institute of Theoretical and Experimental Physics,*

B. Chermushkinskaya 25, 117218 Moscow, Russia

²*Joint Institute for Nuclear Research, 141980 Dubna, Russia*

Abstract

The double beta decay experiment NEMO 3 has been taking data since February 2003. The aim of this experiment is to search for neutrinoless ($0\nu\beta\beta$) decay and investigate two neutrino double beta decay in seven different isotopically enriched samples (^{100}Mo , ^{82}Se , ^{48}Ca , ^{96}Zr , ^{116}Cd , ^{130}Te and ^{150}Nd). After analysis of the data corresponding to 3.75 y, no evidence for $0\nu\beta\beta$ decay in the ^{100}Mo and ^{82}Se samples was found. The half-life limits at the 90% C.L. are $1.1 \cdot 10^{24}$ y and $3.6 \cdot 10^{23}$ y, respectively. Additionally for $0\nu\beta\beta$ decay the following limits at the 90% C.L. were obtained, $> 1.3 \cdot 10^{22}$ y for ^{48}Ca , $> 9.2 \cdot 10^{21}$ y for ^{96}Zr and $> 1.8 \cdot 10^{22}$ y for ^{150}Nd . The $2\nu\beta\beta$ decay half-life values were precisely measured for all investigated isotopes.

PACS numbers: 23.40.-s, 14.60.Pq

*Electronic address: barabash@itep.ru

I. INTRODUCTION

Interest in neutrinoless double-beta decay has seen a significant renewal in recent years after evidence for neutrino oscillations was obtained from the results of atmospheric, solar, reactor and accelerator neutrino experiments (see, for example, the discussions in [1–3]). These results are impressive proof that neutrinos have a non-zero mass. However, the experiments studying neutrino oscillations are not sensitive to the nature of the neutrino mass (Dirac or Majorana) and provide no information on the absolute scale of the neutrino masses, since such experiments are sensitive only to the difference of the masses, Δm^2 . The detection and study of $0\nu\beta\beta$ decay may clarify the following problems of neutrino physics (see discussions in [4–6]): (i) lepton number non-conservation, (ii) the nature of the neutrino (Dirac or Majorana particle), (iii) absolute neutrino mass scale (a measurement or a limit on m_1), (iv) the type of neutrino mass hierarchy (normal, inverted, or quasidegenerate), (v) CP violation in the lepton sector (measurement of the Majorana CP-violating phases).

The currently running NEMO 3 experiment is devoted to the search for $0\nu\beta\beta$ decay and to the accurate measurement of two neutrino double beta decay ($2\nu\beta\beta$ decay) by means of the direct detection of the two electrons. This tracking experiment, in contrast to experiments with ^{76}Ge , detects not only the total energy deposition, but other parameters of the process. These include the energy of the individual electrons, angle between them, and the coordinates of the event in the source plane. Since June of 2002, the NEMO 3 detector has operated in the Fréjus Underground Laboratory (France) located at a depth of 4800 m w.e. Then in February 2003, after the final tuning of the experimental set-up, NEMO 3 has been taking data devoted to double beta decay studies. The first results with ^{100}Mo , ^{82}Se , ^{150}Nd and ^{96}Zr were published in [7–12].

II. NEMO-3 EXPERIMENT

The NEMO 3 detector has three main components, a foil consisting of different sources of double beta decay isotopes and copper, a tracker made of Geiger wire cells and a calorimeter made of scintillator blocks with PMT readout, surrounded by a solenoidal coil. The detector has the ability to discriminate between events of different types by positive identification of charged tracks and photons. A schematic view of the NEMO 3 detector is shown in Fig. 1.

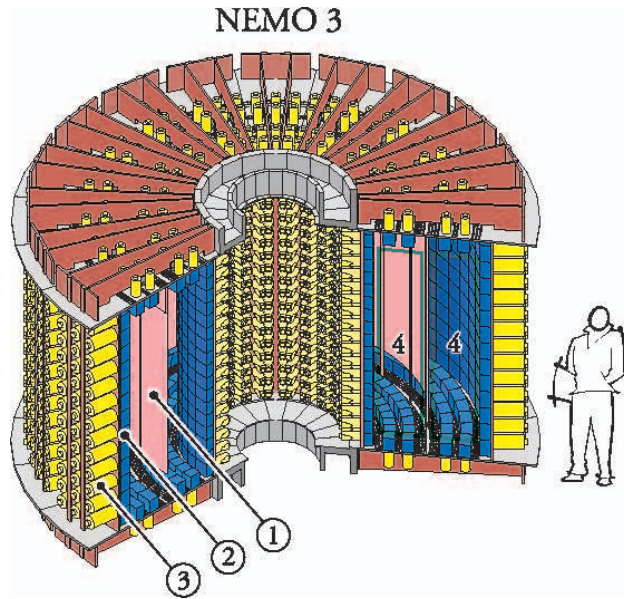


FIG. 1: The NEMO-3 detector without shielding. 1 – source foil; 2– plastic scintillator; 3 – low radioactivity PMT; 4 – tracking chamber.

The NEMO 3 detector is cylindrical in design and is composed of twenty equal sectors. The external dimensions of the detector with shields are 6 m in diameter and 4 m in height. NEMO 3 is based on the techniques tested on previous incarnations of the experiment NEMO 1 [13], and NEMO 2 [14].

The wire chamber is made of 6180 open octagonal drift cells which operate in Geiger mode (Geiger cells). A gas mixture of $\sim 95\%$ helium, 4% ethyl-alcohol, 1% argon and 0.15% water at 10 mbar above atmospheric pressure is used as the filling gas of the wire chamber. Each drift cell provides a three-dimensional measurement of the charged particle tracks by recording the drift time and the two plasma propagation times. The transverse position is determined from the drift time, while the longitudinal position is deduced from the difference between the plasma propagation times at both ends of the cathode wires. The average vertex position resolution for the two-electron events is $\sigma_t = 0.5$ cm in the transverse plane of the detector and $\sigma_l = 0.8$ cm in the longitudinal plane. The Geiger cell information is treated by the track reconstruction program based on the cellular automaton algorithm, described in [15].

The calorimeter, which surrounds the wire chamber, is composed of 1940 plastic scintillator blocks coupled by light-guides to very low-radioactivity photomultiplier tubes (PMTs)

TABLE I: Investigated isotopes with NEMO 3 [17]

Isotope	^{100}Mo	^{82}Se	^{130}Te	^{116}Cd	^{150}Nd	^{96}Zr	^{48}Ca
Enrichment, %	97	97	89	93	91	57	73
Mass of isotope, g	6914	932	454	405	36.6	9.4	7.0

developed by Hammamatsu. The energy resolution FWHM of the calorimeter ranges from 14.1 to 17.6% for 1 MeV electrons, while the time resolution is 250 ps at 1 MeV.

The apparatus accommodates almost 10 kg of different double beta decay isotopes (see Table 1). Most of these isotopes are highly enriched and all are shaped in the form of thin metallic or composite foils with a density of 30-60 mg/cm². Three sectors are used for external background measurements and are equipped respectively with pure Cu (one sector, 621 g) and natural Te (1.7 sectors, 614 g of $^{nat}\text{TeO}_2$). Some of the sources, including ^{100}Mo , have been purified in order to reduce their content of ^{208}Tl (from ^{232}Th and ^{228}Th , and from ^{228}Ra with a half-life of 5.75 y) and ^{214}Bi (from ^{226}Ra with a half-life of 1600 y) either by a chemical procedure [16], or by a physical procedure [17]. The foils were placed inside the wire chamber in the central vertical plane of each sector. The majority of the detector, 12 sectors, notes a total of 6.9 kg of ^{100}Mo .

The detector is surrounded by a solenoidal coil which generates a vertical magnetic field of 25 Gauss inside the wire chamber. This magnetic field allows electron-positron identification by measuring the curvature of their tracks. The ambiguity of the e^+/e^- recognition based on the curvature reconstruction is 3% at 1 MeV.

The whole detector is covered by two types of shielding against external γ -rays and neutrons. The inner shield is made of 20 cm thick low-radioactivity iron which stops γ -rays and slow neutrons. The outer shield is comprised of tanks filled with borated water on the vertical walls and wood on the top and bottom designed to thermalize and capture neutrons.

At the beginning of the experiment, the radon inside the tracking chamber, and more precisely its decay product, ^{214}Bi present in its radioactive chain, was found to be the

predominant background. Radon is present in the air of the laboratory and originates from the rock surrounding. It can penetrate the detector through small leaks. A tent coupled to a radon-free air factory was installed around the detector in October 2004 in order to decrease the presence of radon inside the tracker.

Since February 2003, after the final tuning of the experimental set-up, NEMO 3 has routinely been taking data devoted to double beta decay studies. The calibration with radioactive sources is carried out every six weeks. The stability of the calorimeter is checked daily with a laser based calibration system [17].

The advantage of the NEMO 3 detector rests in its capability to identify the two electrons from $\beta\beta$ decay and the de-excitation photons from the excited state of the daughter nucleus. The NEMO 3 calorimeter also measures the detection time of the particles. The use of appropriate time-of-flight (TOF) cuts, in addition to energy cuts, allows for an efficient reduction of all backgrounds.

A full description of the detector and its characteristics can be found in [17].

III. EXPERIMENTAL RESULTS

The $\beta\beta$ events are selected by requiring two reconstructed electron tracks with a curvature corresponding to a negative charge and originating from a common vertex in the source foil. The energy of each electron measured in the calorimeter should be greater than 200 keV. Each track must hit a separate scintillator block. No trackless PMT signals are allowed. The event is recognized as internal using the measured time difference of the two PMT signals compared to the estimated time-of-flight difference of the electrons.

The background can be classified into three groups: external γ -rays, radon inside the tracking volume and internal radioactive contamination of the source. All three were estimated from NEMO 3 data with events of various topologies [18]. In particular the radon and internal ^{214}Bi is measured with $e\gamma\alpha$ events. The $e\gamma$, $e\gamma\gamma$ and $e\gamma\gamma\gamma$ events are used to measure the ^{208}Tl activity requiring the detection of the 2.65 MeV γ -ray typical of the ^{208}Tl β -decay. Single electron events are used to measure the foil contamination by β -emitters. The external background is measured with the events with the detected incoming γ -rays that produce an electron in the source foil. The control of the external background is done with two-electron events originating from the pure Copper and natural Tellurium foils. Mea-

TABLE II: Two neutrino half-life values for different nuclei obtained in the NEMO 3 experiment (for ^{116}Cd , ^{48}Ca and ^{130}Te the results are preliminary). The first error is statistical and the second is systematic while S/B is the signal-to-background ratio.

Isotope	Measurement time, days	Number of 2ν events	S/B	$T_{1/2}(2\nu)$, y
^{100}Mo	389	219000	40	$(7.11 \pm 0.02 \pm 0.54) \times 10^{18}$ [8]
^{100}Mo - $^{100}\text{Ru}(0_1^+)$	334.3	37.5	4	$(5.7_{-0.9}^{+1.3} \pm 0.8) \times 10^{20}$ [10]
^{82}Se	389	2750	4	$(9.6 \pm 0.3 \pm 1.0) \times 10^{19}$ [8]
^{116}Cd	168.4	1371	7.5	$(2.8 \pm 0.1 \pm 0.3) \times 10^{19}$
^{96}Zr	1221	428	1	$(2.35 \pm 0.14 \pm 0.19) \times 10^{19}$ [12]
^{150}Nd	939	2018	2.8	$(9.11_{-0.22}^{+0.25} \pm 0.63) \times 10^{18}$ [11]
^{48}Ca	943.16	116	6.8	$(4.4_{-0.4}^{+0.5} \pm 0.4) \times 10^{19}$
^{130}Te	1152	236	0.35	$(6.9 \pm 0.9 \pm 1.0) \times 10^{20}$

measurements performed with HPGe detectors and with radon detectors are used to verify the results. Different level of radon activity in the tracking volume were detected in the data taken before October 2004 (Phase 1), and after the installation of the antiradon facility (Phase 2).

A. Measurement of $2\nu\beta\beta$ half-lives

Measurements of the $2\nu\beta\beta$ decay half-lives have been performed for seven isotopes available in NEMO 3 (see Table 1). The NEMO 3 results of $2\nu\beta\beta$ half-life measurements are given in Table 2. For all the isotopes the energy sum spectrum, single-electron energy spectrum and angular distribution were measured. The ^{100}Mo double beta decay to the 0_1^+ excited state of ^{100}Ru $T_{1/2}^{2\nu} = [5.7_{-0.9}^{+1.3}(\text{stat}) \pm 0.8(\text{syst})] \cdot 10^{20}\text{y}$ has also been measured by NEMO 3 [10]. For ^{100}Mo , ^{82}Se , ^{96}Zr and ^{150}Nd these results are published. For the other isotopes their status is preliminary.

B. Search for $0\nu\beta\beta$ decay

No evidence for $0\nu\beta\beta$ decay was found for all seven isotopes. The associated limits are presented in Table 3.

TABLE III: Limits at 90% C.L. on $0\nu\beta\beta$ decay (neutrino mass mechanism) for different nuclei obtained in the NEMO 3 experiment.

Isotope	Measurement time, days	$T_{1/2}(0\nu)$, y
^{100}Mo	1409	$> 1.1 \cdot 10^{24}$ y
^{82}Se	1409	$> 3.6 \cdot 10^{23}$ y
^{130}Te	1221	$> 1 \cdot 10^{23}$ y
^{150}Nd	939	$> 1.8 \cdot 10^{22}$ y
^{116}Cd	77	$> 1.6 \cdot 10^{22}$ y
^{48}Ca	943.16	$> 1.3 \cdot 10^{22}$ y
^{96}Zr	1221	$> 9.2 \cdot 10^{21}$ y

The $0\nu\beta\beta$ -decay search in NEMO 3 is most promising with ^{100}Mo and ^{82}Se because of the larger available sample mass and high enough $Q_{\beta\beta} \sim 3$ MeV. The data taken from February 2003 till the end of 2008 has been used in the search for neutrinoless double beta decay. The data corresponds to 1409 effective days of data collection. For the case of the mass mechanism, the $0\nu\beta\beta$ -decay signal is expected to be a peak in the energy sum distribution at the position of the transition energy $Q_{\beta\beta}$. The two-electron energy sum spectra for ^{100}Mo and ^{82}Se are shown in Fig. 2 and Fig. 3 demonstrating a good agreement between observed and expected number of events.

Since no excess is observed at the tail of the distributions, limits are set on the neutrinoless double beta decay with the CL_s method based on the use of a log-likelihood ratio (LLR) test statistics [19]. This gives the lower limits on the half-life of $T_{1/2}^{0\nu}(^{100}\text{Mo}) > 1.1 \cdot 10^{24}\text{yr}$ (90% C.L.) and $T_{1/2}^{0\nu}(^{82}\text{Se}) > 3.6 \cdot 10^{23}\text{yr}$ (90% C.L.) A lower half-life limit translates into an upper limit on the effective Majorana neutrino mass $\langle m_\nu \rangle$. According to the recent results of different theoretical NME calculations (see Table 4) the half-life limit obtained for ^{100}Mo

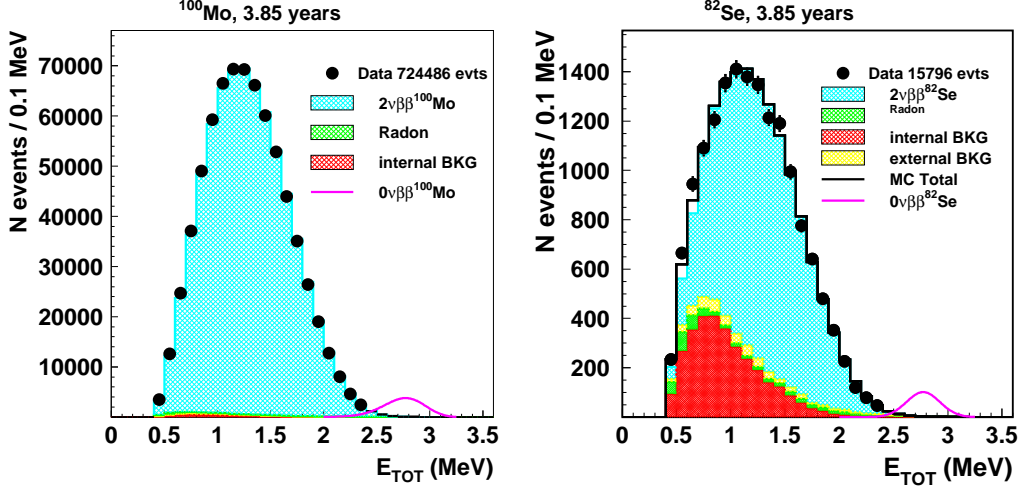


FIG. 2: Distribution of the energy sum of two electrons for ^{100}Mo (left) and ^{82}Se (right), 1409 d data. The shape of a hypothetical 0ν signal is shown by the curve in arbitrary units.

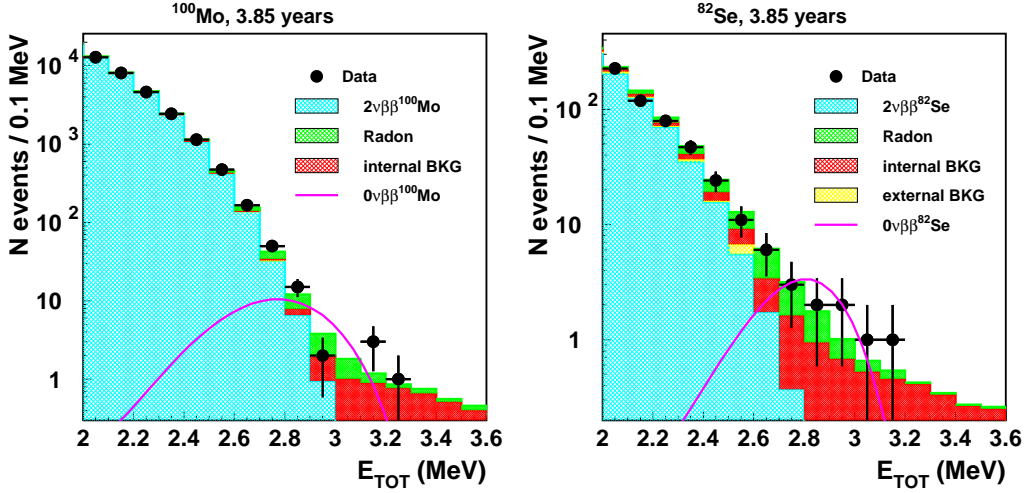


FIG. 3: Distribution of the energy sum of two electrons in the region around $Q_{\beta\beta}$ value for ^{100}Mo (left) and ^{82}Se (right), 1409 d data. High energy tail of the energy sum distribution for events in molybdenum (left) and selenium (right) foils are shown with black points. The background contributions are shown within the histogram. The shape of a hypothetical 0ν signal is shown by the curve in arbitrary units.

corresponds to the neutrino mass interval $\langle m_\nu \rangle < 0.45 - 0.93$ eV. It is less restrictive for ^{82}Se $\langle m_\nu \rangle < 0.89 - 2.43$ eV. The reached NEMO 3 sensitivity on the neutrino mass is close to that of IGEX [20], the Heidelberg-Moscow collaboration [21] and CUORICINO [22].

TABLE IV: Limits on the effective neutrino mass $\langle m_\nu \rangle$ (in eV) corresponding to different theoretical model calculations of nuclear matrix elements obtained for $T_{1/2}(0\nu\beta\beta) > 1.1 \cdot 10^{24}$ y in case of ^{100}Mo and $T_{1/2}(0\nu\beta\beta) > 3.6 \cdot 10^{23}$ y in case of ^{82}Se .

Nuclear matrix elements		^{100}Mo	^{82}Se
Shell model	[23]	-	< 2.43
QRPA	[24],[25]	$< 0.58 - 0.75$	$< 1.12 - 1.38$
QRPA	[26]	$< 0.45 - 0.93$	$< 0.89 - 1.61$
IBM-2	[27]	$< 0.49 - 0.55$	$< 1.03 - 1.19$
PHFB	[28]	< 0.70	

C. Search for double beta decay with Majoron emission

The $0\nu\chi^0\beta\beta$ decay requires the existence of a Majoron. It is a massless Goldstone boson that arises due to a global breakdown of $(B-L)$ symmetry, where B and L are, respectively, the baryon and the lepton number. The Majoron, if it exists, could play a significant role in the history of the early Universe and in the evolution of stars. A 2β -decay model that involves the emission of two Majorons was proposed within supersymmetric theories and several other models of the Majoron were proposed in the 1990s (see review [29] and references therein). The possible two electrons energy spectra for different $0\nu\chi^0\beta\beta$ decay modes of ^{100}Mo are shown in Fig. 4. Here n is the spectral index, which defines the shape of the spectrum. For example, for an ordinary Majoron $n = 1$, for 2ν decay $n = 5$, in the case of a bulk Majoron $n = 2$ and for the process with two Majoron emission $n = 3$ or 7.

No evidence for $0\nu\chi^0\beta\beta$ decay was found for all seven isotopes. The limits for ^{100}Mo , ^{82}Se , ^{150}Nd and ^{96}Zr are presented in Table 5. In particular, strong limits on "ordinary" Majoron (spectral index 1) decay of ^{100}Mo ($T_{1/2} > 2.7 \cdot 10^{22}$ y) and ^{82}Se ($T_{1/2} > 1.5 \cdot 10^{22}$ y) have been obtained. Corresponding bounds on the Majoron-neutrino coupling constant are $\langle g_{ee} \rangle < (0.35 - 0.85) \cdot 10^{-4}$ and $< (0.6 - 1.9) \cdot 10^{-4}$, respectively (using nuclear matrix elements from [23–28]).

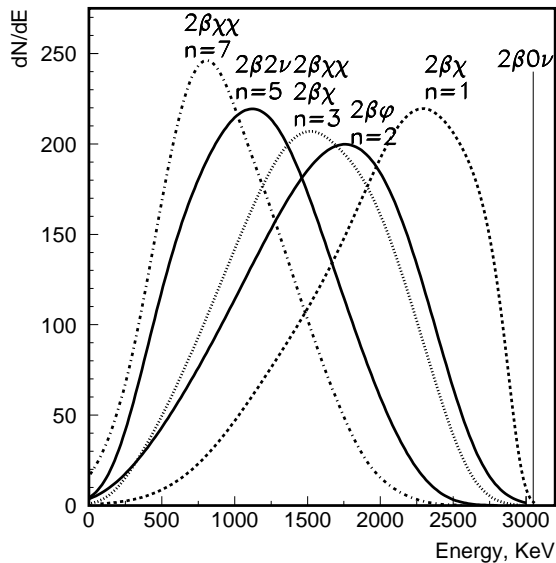


FIG. 4: Energy spectra of different modes of $2\beta 2\nu$ ($n = 5$), $2\beta\chi^0$ ($n = 1, 2$ and 3) and $2\beta\chi^0\chi^0$ ($n = 3$ and 7) decays of ^{100}Mo (see text).

TABLE V: NEMO 3 limits on $T_{1/2}$ (y) for decay with one and two Majorons at 90% C.L. for modes with spectral index $n = 1, n = 2, n = 3$ and $n = 7$.

Isotope	$n = 1$	$n = 2$	$n = 3$	$n = 7$
^{100}Mo [8]	$>2.7 \cdot 10^{22}$	$>1.7 \cdot 10^{22}$	$>1 \cdot 10^{22}$	$>7 \cdot 10^{19}$
^{82}Se [8]	$>1.5 \cdot 10^{22}$	$>6 \cdot 10^{21}$	$>3.1 \cdot 10^{21}$	$>5 \cdot 10^{20}$
^{96}Zr [12]	$>1.9 \cdot 10^{21}$	$>9.9 \cdot 10^{20}$	$>5.8 \cdot 10^{20}$	$>1.1 \cdot 10^{20}$
^{150}Nd [11]	$>1.5 \cdot 10^{21}$	$>5.4 \cdot 10^{20}$	$>2.2 \cdot 10^{20}$	$>4.7 \cdot 10^{19}$

IV. CONCLUSION

The NEMO 3 detector has been operating within its target performance specifications since February 2003. The $2\nu\beta\beta$ decay has been measured for seven isotopes with high statistics and greater precision than previously. The ^{100}Mo $2\nu\beta\beta$ decay to the 0_1^+ excited state of ^{100}Ru has also been measured. No evidence for $0\nu\beta\beta$ decay was found for all seven isotopes. The best $0\nu\beta\beta$ limits have been obtained with ^{100}Mo ($> 1.1 \cdot 10^{24}$ y at 90% C.L.)

and ^{82}Se ($> 3.6 \cdot 10^{23}$ y at 90% C.L.).

NEMO 3 is current experiment with data collection continued into ~ 2011 .

Acknowledgements

The authors thank the Modane Underground Laboratory staff for their technical assistance in running the experiment. This work was supported by grants from RFBR (no 06-02-72553 and no 09-02-92676) and with support from the Russian Federal Agency for Atomic Energy.

-
- [1] J. W. F. Valle, hep-ph/0608101.
 - [2] S. M. Bilenky, J. Phys. A **40**, 6707 (2007).
 - [3] R. N. Mohapatra and A. Y. Smirnov, Ann. Rev. Nucl. Part. Sci. **56**, 569 (2006).
 - [4] S. Pascoli, S. T. Petcov, and W. Rodejohann, Phys. Lett. B **558**, 141 (2003).
 - [5] R. N. Mohapatra *et al.*, hep-ph/0510213.
 - [6] S. Pascoli, S. T. Petcov, and T. Schwetz, Nucl. Phys. B **734**, 24 (2006).
 - [7] R. Arnold *et al.*, JETP Lett. **80**, 377 (2004).
 - [8] R. Arnold *et al.*, Phys. Rev. Lett. **95**, 182302 (2005).
 - [9] R. Arnold *et al.*, Nucl. Phys. A **765**, 483 (2006).
 - [10] R. Arnold *et al.*, Nucl. Phys. A **781**, 209 (2007).
 - [11] J. Argyriades *et al.*, Phys. Rev. C **80**, 032501R (2009).
 - [12] J. Argyriades *et al.*, nucl-ex/0906.2694.
 - [13] D. Dassié *et al.*, Nucl. Instrum. Methods A **309**, 465 (1991).
 - [14] R. Arnold *et al.*, Nucl. Instrum. Methods A **354**, 338 (1995).
 - [15] I. Kisel *et al.*, Nucl. Instrum. Methods A **384**, 433 (1997).
 - [16] R. Arnold *et al.*, Nucl. Instrum. Methods A **474**, 93 (2001).
 - [17] R. Arnold *et al.*, Nucl. Instrum. Methods A **536**, 79 (2005).
 - [18] R. Arnold *et al.*, Nucl. Instrum. Methods A **606**, 449 (2009).
 - [19] W. Fisher, FERMILAB-TM-2386-E, 2007 (unpublished).
 - [20] C.E. Aalseth *et al.*, Phys. Rev. D **65**, 092007 (2002).

- [21] H.V. Klapdor-Kleingrothaus *et al.*, Eur. Phys. J. A **12**, 147 (2001).
- [22] C. Arnaboldi *et al.*, Phys. Rev. C **78**, 035502 (2008).
- [23] E. Caurier *et al.*, Phys. Rev. Lett. **100**, 052503 (2008).
- [24] M. Kortelainen and J. Suhonen, Phys. Rev. C **76**, 024315 (2007).
- [25] M. Kortelainen and J. Suhonen, Phys. Rev. C **75**, 051303(R) (2007).
- [26] F. Simkovic *et al.*, Phys. Rev. C **77**, 045503 (2008).
- [27] J. Barea and F. Iachello, Phys. Rev. C **79**, 044301, (2009).
- [28] K. Chaturvedi *et al.*, Phys. Rev. C **78**, 054302 (2008).
- [29] A.S. Barabash, Phys. At. Nucl. **73**, 162 (2010); hep-ex/0807.2948.